Cardiac arrhythmia classification using machine learning

Master's thesis in Complex Adaptive Systems

ADAM SÖDERHOLM

DEPARTMENT OF PHYSICS

CHALMERS UNIVERSITY OF TECHNOLOGY
Gothenburg, Sweden 2023
www.chalmers.se

Master's thesis 2023

Cardiac arrhythmia classification using machine learning

ADAM SÖDERHOLM

CHALMERS
UNIVERSITY OF TECHNOLOGY

Department of Physics
Chalmers University of Technology
Gothenburg, Sweden 2023

Cardiac arrhythmia classification using machine learning
ADAM SÖDERHOLM

Supervisor: Gustav Karlsson, Triathlon Group
Examiner: Mats Granath, Department of Physics

Master's Thesis 2023
Department of Physics
Chalmers University of Technology
SE-412 96 Gothenburg
Telephone +46 31 772 1000

Typeset in LaTeX
Printed by Chalmers Reproservice
Gothenburg, Sweden 2023

Cardiac arrhythmia classification using machine learning
ADAM SÖDERHOLM
Department of Physics
Chalmers University of Technology

Abstract

Machine learning models interpreting ECG signals enable scalability to increase the number of patients examined for cardiac arrhythmia and hence contribute to democratize healthcare. In this thesis a machine learning model for detecting ectopic heartbeat arrhythmias is developed and evaluated. The initial aim was to interpret signals from mobile ECG devices but due to lack of data, the model was developed and evaluated on the publicly available MIT-BIH Arrhythmia Database. The evaluation followed an inter-patient evaluation scheme to mimic the performance of the model in real-world clinical settings. The proposed model design included ensemble learning between a convolutional neural network and a multilayer perceptron network. The model was able to detect non-ectopic, supraventricular ectopic, and ventricular ectopic heartbeats with a recall of 97 %, 62 %, and 78 %, respectively.

Keywords: Arrhythmia, electrocardiogram, machine learning, convolutional neural network, multilayer perceptron network, ensemble learning

Acknowledgments

Thank you to Mats Granath for being the examiner of this Master's thesis. Your guidance and insights have been valuable for my work.

Thank you to Gustav Karlsson for being my supervisor. Our discussions on how to perform and structure this project have been a valuable guidance.

Thank you to Viking Zandhoff Westerlund for being the opponent of this thesis. It was improved thanks to your suggestions and interest.

Finally, I would like to thank the collaboration company for the opportunity to do my thesis within this interesting research area.

Adam Söderholm, Gothenburg, June 2023

Contents

List of Acronyms

Below is the list of acronyms that have been used throughout this thesis listed in alphabetical order:

AAMI	Association for the Advancement of Medical Instrumentation
AV	Atrioventricular
CNN	Convolutional neural network
ECG	Electrocardiogram
FDA	U.S. Food and Drug Administration
MLII	Modified limb lead II
N	Non-ectopic
PCA	Principal component analysis
S	Supraventricular ectopic
SA	Sinoatrial
T-SNE	T-distributed Stochastic Neighbor Embedding
V	Ventricular ectopic
WHO	World Health Organization

List of Figures

List of Tables

1

Introduction

Cardiovascular diseases, a group of disorders affecting the heart or blood vessels, are the leading cause of death worldwide. In 2019 the World Health Organization (WHO) estimated that 17.9 million people died from cardiovascular diseases which represent 32 % of all deaths [1]. Most deaths caused by cardiovascular diseases occur in low- and middle-income countries. In general, the population in low- and middle-income countries does not have the benefit of primary healthcare services, crucial for detecting and treating cardiovascular diseases [1]. This raises the question of whether technology has the possibility to increase the availability of care and the number of examined patients and thereby democratize healthcare.

1.1 Background

Electrocardiogram (ECG) has helped cardiologists to detect cardiovascular diseases for decades and is today one of the most utilized tools for medical practices [2], [3]. Not only cardiologists but also doctors of various specialties, nurses, and physiologists are interpreting ECG signals to determine medical treatment for patients. The interpretation of an ECG signal is a complex task and inaccurate evaluation can have fatal consequences due to the risk of incorrect treatment [4]. In special cases, patients are monitored by an ECG device for several hours, and cardiologists analyze each individual heartbeat. Hence, manual interpretation of ECG signals is a time-consuming task, and human error, due to fatigue or other factors, increases the number of misdiagnoses [5].

To minimize the number of misdiagnoses, reduce costs and facilitate health care decisions, computer-aided interpretation of ECG signals was introduced over 50 years ago. Today millions of ECG signals are recorded annually and most of them are interpreted automatically. For professionals in the healthcare domain, the computer-aided interpretation of ECG signals has served as a crucial adjunct in many clinical settings. However, despite the technical evolution, computer-aided systems are still producing incorrect interpretations which results in misdiagnoses [6].

Recent studies indicate that continuous monitoring of the heart's activity can help to detect cardiovascular diseases. As a result, the number of mobile ECG devices, which can be worn by patients in everyday life for a longer period than what is

normally measured at a hospital is expanding rapidly. Companies are gathering ECG signals from wearables and pocket devices to detect patients' abnormal heartbeats and rhythms. Due to technical diversities and hardware differences in mobile ECG devices, difficulties in interpreting such signals increase [7]. The diversity and increased volume of mobile ECG devices enlarge the demand for high-performing computer-aided systems.

Mobile devices for ECG monitoring together with improved computer-aided interpretation have the potential to increase the number of monitored patients and avoid misdiagnoses due to human error. Hence, mobile ECG devices together with state-of-art machine learning enable scalability to democratize healthcare [8]. The potential of identifying cardiovascular diseases from ECG signals using machine learning interpretation is investigated in this thesis.

1.2 Aim

The aim of this thesis is to develop, train and evaluate a machine learning model for classifying single heartbeat arrhythmias from ECG signals. This is preparation for the model to interpret signals from the mobile ECG device manufactured by the collaboration company.

1.3 Limitations

The initial aim was to interpret signals from a mobile ECG device manufactured by the collaboration company but due to lack of data, the model was developed and evaluated on a public dataset.

Rhythmic arrhythmias will not be detected nor classified by the machine learning model. See Section 2.3 for definitions of single heartbeat and rhythmic arrhythmias.

There are several types of single heartbeat arrhythmias. This thesis is limited to only classify heartbeats into three categories, non-ectopic, supraventricular ectopic and ventricular ectopic heartbeats. See Section 2.3.

1.4 Related work

Using machine learning to detect arrhythmias in ECG signals is a well-known field of study and several researchers have published papers within this topic. Various deep learning techniques such as long short-term memory networks, recurrent neural networks, and convolutional neural networks have been used for this purpose [9].

In a study performed by Hannun *et al.* [6] in collaboration with Stanford University, a deep neural network was developed to detect arrhythmias. The objective of this study was to detect rhythmic arrhythmias and compare the model's performance to cardiologists' performance. The data consisted of ECG signals from 53 549 patients

recorded from a single-lead ambulatory ECG monitoring device. The algorithm was able to classify twelve different types of rhythmic arrhythmias and achieved an F1 score of 83.7 % outperforming cardiologists' F1 score of 78.0 %.

In research performed by Sellami and Hwang [10] a similar network architecture as Hannun *et al.* developed was used to detect single heartbeat arrhythmias. In this study, ECG signals from the MIT-BIH Arrhythmia Database were used. Significant for the study was their suggested batch-weighted loss function to overcome the challenges of the imbalanced data. Another notable initiative of the study was the purpose of using multiple individual heartbeats as input to the network to increase performance. The network achieved an accuracy of 99.48 % and 88.34 % using an intra-patient and inter-patient paradigm respectively.

2

Medical theory

This chapter presents medical theory relevant for understanding the work performed during this project. A brief introduction to the cardiac conduction system, arrhythmias, and ECGs are presented. Additionally, regulations for evaluating algorithmic classification of cardiac arrhythmias are listed.

2.1 Cardiac conduction system

The contraction of the heart is caused by electrical impulses conducted through the cardiac conduction system. Electrical impulses occur on a cellular level due to ion concentration differences between the cell and its surrounding which causes an action potential. The rise of an action potential is called depolarization while the opposite, the return of a potential, is called repolarization [11].

Electrical impulses originate from the sinoatrial (SA) node which is located in the upper part of the heart's right atrium. The impulse conducts through the atria, forcing them to contract, and thereby push blood into the ventricles [12]. The contraction of the atria is shown on an ECG as the P wave, atrial depolarization, see Figure 2.1 [13].

Thereafter, the atrioventricular (AV) node receives and delays the electrical impulse originating from the SA node. The delay ensures that the contraction of the atria is complete and is important for a successful ventricular filling [12].

After the delay at the AV node, the electrical impulse reaches the His-Purkinje system which consists of the bundle of His and the Purkinje fibers. The impulse conducts through the bundle of His to the Purkinje fibers which deliver the electrical impulse to the ventricles, forcing them to contract [12]. The contraction of the ventricles is shown on an ECG as the QRS complex. Finally, repolarization of the ventricles occurs which corresponds to the T wave in an ECG, see Figure 2.1. Atrial repolarization coincides with the QRS complex and is therefore not distinguishable in an ECG pattern [13].

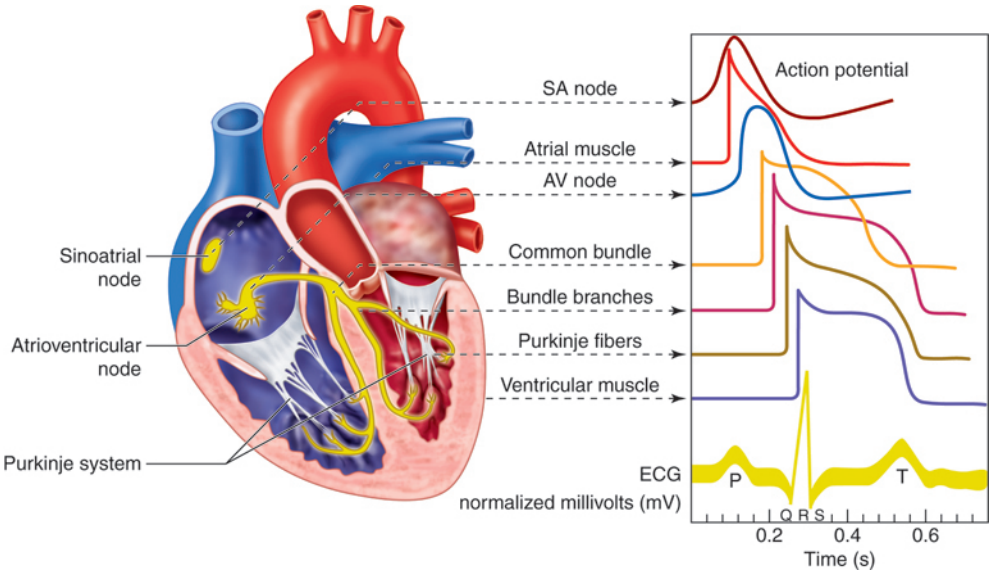

Figure 2.1: Anatomy of the heart and electrical activity of a heartbeat. From [14] CC BY-SA 4.0.

2.2 Electrocardiogram

The function of an ECG is to record the electrical activity of the heart during the cardiac conduction cycle. The change of ion concentration during depolarization and repolarization results in an electrical activity that can be recorded by an ECG [15]. A healthy ECG pattern of the electrical activity during a heartbeat with P wave, QRS complex, and T wave is illustrated in Figure 2.2.

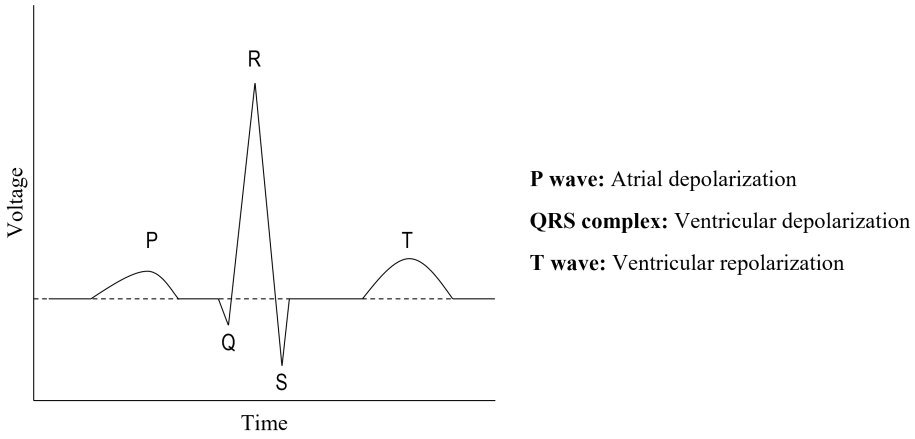

Figure 2.2: Illustration of an ECG pattern during a normal heartbeat.

The ECG examination is performed by attaching electrodes to the skin of the patient to measure electrical currents. Traditionally, in a 12-lead ECG, 10 electrodes are attached. By analyzing these 10 electrodes, 12 graphical descriptions (leads) of the heart's electrical activity can be measured and visualized [16].

Since ECG is a non-invasive and highly accessible technology it plays a crucial role in detecting cardiac diseases. By analyzing electrical signals it is possible to detect abnormalities in the heart's function. Each type of arrhythmia is associated with a specific pattern of the visualized electrical activity and can therefore be identified and diagnosed by analyzing the ECG signals [5].

2.3 Arrhythmias

Arrhythmia is a condition describing an abnormal heartbeat or rhythm [17]. Arrhythmias can be divided into two categories. The first category includes abnormalities of a single heartbeat, herein called single heartbeat arrhythmia. The second category consists of a sequence of irregular heartbeats changing the heart's rhythm, herein called rhythmic arrhythmias [5].

One type of single heartbeat arrhythmias is ectopic heartbeats. An ectopic heartbeat occurs when the electrical impulse causing the heart to contract does not originate from the SA node. Depending on where the electrical impulse originates, ectopic heartbeats can be categorized into supraventricular ectopic heartbeat, where the impulse originates from the atria, and ventricular ectopic heartbeat, where the impulse originates from the ventricles [18].

An ectopic heartbeat can be detected and identified by analyzing an ECG signal since the electrical impulse does not follow the normal sequence of the cardiac conduction cycle. The contraction of an ectopic heartbeat most often occurs earlier than expected and appears on an ECG as a deviation in shape and time between QRS complexes [19]. Figure 2.3 illustrates ECG signals of non-ectopic, supraventricular ectopic, and ventricular ectopic heartbeats.

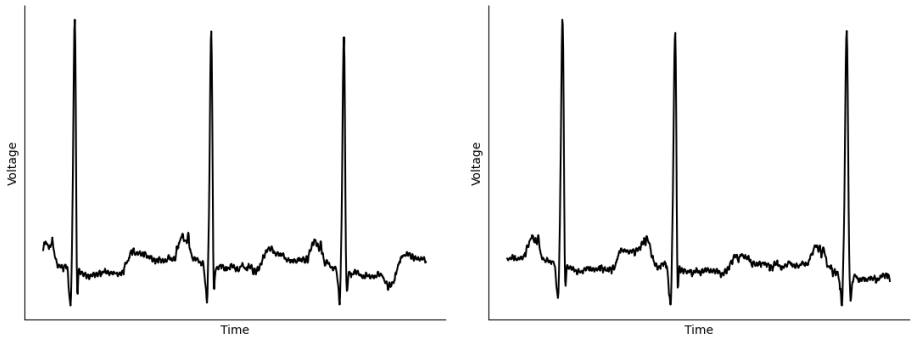

(a) Non-ectopic heartbeats

(b) Middle heartbeat illustrate a supraventricular ectopic heartbeat.

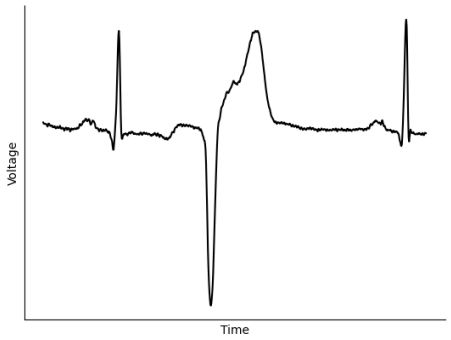

(c) Middle heartbeat illustrate a ventricular ectopic heartbeat

Figure 2.3: Illustration of ectopic heartbeat arrhythmias. Plot of data from the MIT-BIH Arrhythmia Database [20], [21].

While most arrhythmias are harmless some can have fatal consequences. At a crucial level, arrhythmias can either be life threatening or non-life threatening [22]. Ectopic heartbeats are most often harmless and do not require any medical treatment. Anxiety, stress, alcohol, and caffeine increase the risk of ectopic heartbeats and healthcare providers may recommend lifestyle changes for patients [19].

2.4 Algorithmic ECG interpretation standard

There are several public databases containing ECG signals available online. The U.S. Food and Drug Administration (FDA) recommends that arrhythmia detection algorithms are evaluated according to the ANSI/AAMI EC 57 standard [23]. The standard was developed by the Association for the Advancement of Medical Instrumentation (AAMI). According to AAMI, algorithms should be evaluated on three public databases, the MIT-BIH Arrhythmia Database, the American Heart Association ECG Database, and the MIT-BIH Noise Stress Test Database [24]. Annotations of heartbeats following AAMI are listed in the studies [10], [25], [26], [27] and consist of five super classes, non-ectopic (N), supraventricular ectopic (S), ventricular ectopic (V), fusion (F), and unknown (Q) heartbeats. Table 2.1 presents

the relationship between the annotations in the MIT-BIH Arrhythmia Database and AAMI annotations.

Table 2.1: AAMI annotation of the MIT-BIH Arrhythmia Database.

Heartbeat type	AAMI annotation	Heartbeat type	MIT-BIH Arrhythmia Database
Non-ectopic beats	N	Normal beats	N
		Right bundle branch block beats	R
		Left bundle branch block beats	L
		Atrial escape beats	e
		Nodal (junctional) escape beats	j
Supraventricular ectopic beats	S	Atrial premature beats	A
		Nodal (junctional) premature beats	J
		Aberrated atrial premature beats	a
		Supraventricular premature beats	S
Ventricular ectopic beats	V	Premature ventricular contraction	V
		Ventricular escape beats	E
Fusion beats	F	Fusion of ventricular and normal beats	F
Unknown beats	Q	Paced beats	/
		Fusion of paced and normal beats	f
		Unclassifiable beats	Q

According to the limitations of this project only ECG signals from the MIT-BIH Arrhythmia Database were used to develop and evaluate the model. N, S, and V annotations are used according to the AAMI standard. According to the limitations only non-ectopic or ectopic heartbeats are classified and hence the F and Q classes are not used in the project.

3

Machine learning theory

This chapter presents relevant theories of machine learning topics covered in this project. The theory behind convolutional neural networks, ensemble learning, residual networks, and evaluation of models is presented.

3.1 Convolutional neural networks

Neural networks mimic the architecture and dynamics of neurons in the human brain. The fundamental principle is the same for biological neurons as for artificial neurons, they learn by changing the connections to neighboring neurons and can therefore perform a multitude of information-processing tasks [28].

Convolutional networks have been used within the field of machine learning for decades. The characteristic of a convolutional network is inspired by visual perception and is designed to recognize objects or classify images. An advantage of convolutional networks, compared to fully connected networks, is that they contain fewer weights with the same number of neurons. As a result, the computational complexity decreases and the risk of overfitting the data is reduced [28]. Convolutional networks often consist of convolution layers, pooling layers, and fully connected layers [29].

3.1.1 Convolution layers

The main function of a convolution layer is based on the mathematical operator convolution. A kernel is shifted over the input vector to create an output vector, also known as a feature map. Several kernels with different weights can be convolved over the input data to create several feature maps. To obtain the values of the feature map a non-linear function is also applied. The main purpose of convolving a kernel over the input data is to detect features like corners and edges which are vital for image classification and object recognition [28]. In this project, one-dimensional convolution layers are used. The principle of such layers is illustrated in Figure 3.1.

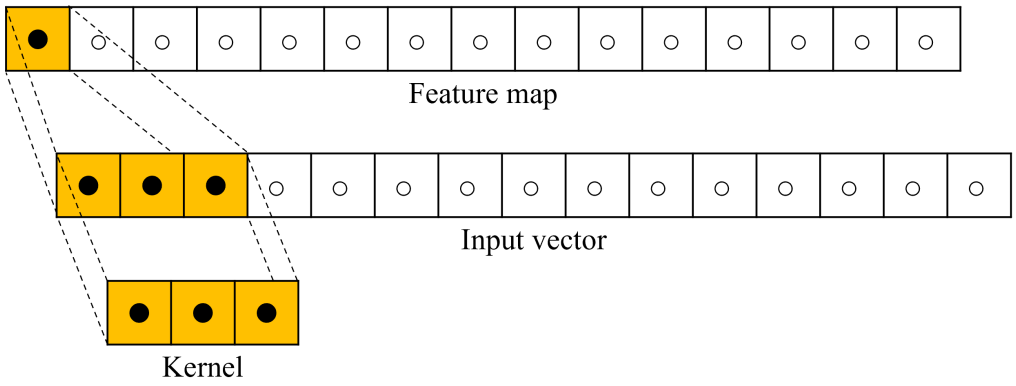

Figure 3.1: Illustration of a convolution layer where a kernel is applied to an input vector to create a feature map.

3.1.2 Pooling layers

A pooling layer is often used to compress the output of a convolution layer. There are different types of pooling units for example max pooling, average pooling, and L_2 pooling to mention a few [28], [29]. In this project, max pooling units are used and the principle of such units is illustrated in Figure 3.2. Traditionally, the pooling operator is not related to any thresholds or weights and does not learn from backpropagation. The pooling window is convolved over the feature maps to compress neighboring neuron values into a single value and hence reduce the size of the feature maps [28]. Pooling layers do therefore reduce the number of variables and thereby increase computational efficiency [29].

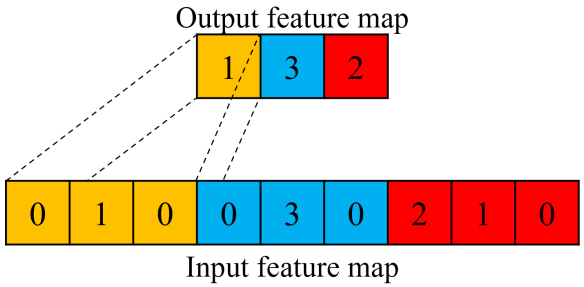

Figure 3.2: Illustration of a pooling layer with max pooling units.

3.1.3 Fully connected layers

In a fully connected layer, every output node from the previous layer is connected to every input node in the next layer [30]. Convolutional neural networks are often designed with a fully connected layer as the final layer to perform classification. The fully connected layer's input is the features extracted by the previous convolution and pooling layers [29].

A neuron's value in a fully connected layer is expressed as,

$$n_i = A(\sum_j w_{ij}x_j - T_i), \tag{3.1}$$

where n_i denotes neuron i in the current layer. w_{ij} expresses the weights from neuron j in the previous layer to neuron i. T_i denotes the threshold for neuron i and A represents an activation function [28]. The architecture of a fully connected layer is illustrated in Figure 3.3.

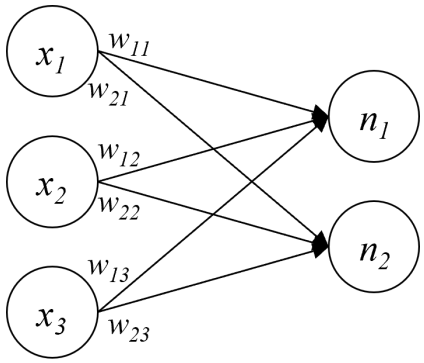

Figure 3.3: Illustration of a fully connected layer.

3.2 Residual networks

For networks with many layers, the change of weights during training becomes smaller close to the input layer because of repeated multiplications of small factors during backpropagation. This is known as the vanishing gradient problem and is a common challenge when training deep neural networks with stochastic gradient descent [28].

To mitigate the vanishing gradient problem residual connections can be introduced to the network. Figure 3.4 illustrate the concept of a residual connection. Such connections introduce an additional path for the data where some layers are skipped to reduce the complexity of the network [28].

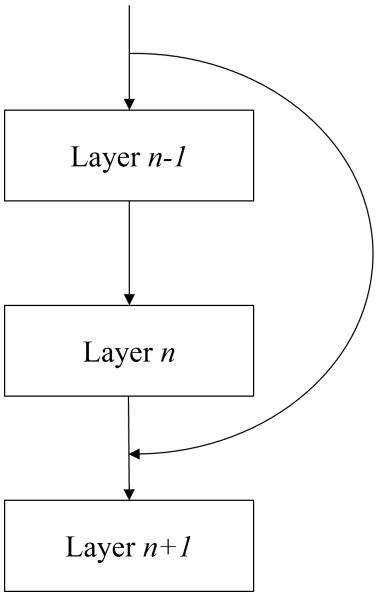

Figure 3.4: Illustration of a network with a residual connection.

3.3 Ensemble learning

A common challenge in machine learning is class imbalance, meaning that one class is considerably larger than all other classes. Machine learning models trained on such data tend to ignore the minority classes. One method to mitigate problems due to class imbalance is to utilize ensemble learning. The main idea behind ensemble learning is that considering several individuals' opinions is better than to only consider one individual's opinion. It mimics human nature to gather and analyze several opinions before making a complex decision [31].

In ensemble learning, predictions from different classifiers are gathered and analyzed before a final prediction is made. There are several methods for how predictions should be combined. Methods where each model individually performs a prediction belong to the independent frameworks. The dependent frameworks are methods where one model's result affects the prediction of another model [31]. The ensemble method used in this project uses an independent framework method and is explained in detail in section 4.5.3. A basic ensemble learning scheme is illustrated in Figure 3.5, where c_1 and c_2 denote two different classifiers.

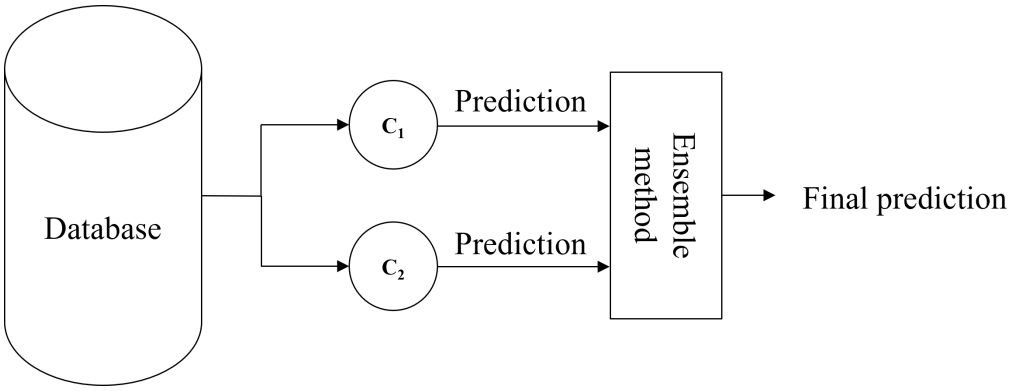

Figure 3.5: Illustration of ensemble learning.

3.4 Evaluation of machine learning models

There are several different metrics to measure the performance of machine learning models. These metrics are most often derived from a confusion matrix. In a confusion matrix, each row represents an actual class label while each column represents a predicted class label. Inserting the model's predictions and the corresponding actual classes into the confusion matrix enables calculations of the model's performance [32].

Table 3.1: Definition of a binary confusion matrix.

		Predicted classes:	
		Positive	Negative
True classes:	Positive	True positive	False negative
	Negative	False positive	True negative

For a binary arrhythmia classification task, a heartbeat can either be normal or abnormal. A true positive (TP) is when the model correctly identifies an abnormal heartbeat while a false negative (FN) is when an abnormal heartbeat is incorrectly predicted as normal. A true negative (TN) is when the model correctly identifies a normal heartbeat while a false positive (FP) is when a normal heartbeat is incorrectly predicted as abnormal [33].

For a multiclass classification task, as the problem in this project, each heartbeat is healthy or belongs to a specific type of arrhythmia. The concept of the confusion matrix is the same, each row represents an actual class label while each column represents a predicted class label. However, the TP, FN, TN, and FP values depend on the class that is being evaluated [34]. Table 3.2 illustrates a multiclass confusion matrix with A as the reference class. When the reference class is changed the

annotations of TP, FN, TN, and FP in the confusion matrix are changed accordingly [34].

Table 3.2: Illustration of a multiclass confusion matrix with A as reference class.

		Predicted classes:		
		A	B	C
True classes:	A	TP	FN	FN
	B	FP	TN	
	C	FP		

This project uses two different metrics to evaluate performance, precision and recall. Precision and recall for class i in a multiclass classification task are defined as [34],

$$Precision_i = \frac{TP_i}{TP_i + FP_i}. \tag{3.2}$$

$$Recall_i = \frac{TP_i}{TP_i + FN_i}. \tag{3.3}$$

4

System development

The development of the arrhythmia detection machine learning model followed an iterative process. This chapter describes the procedure of the development, partial results required for the iterative process, and present key findings.

4.1 Literature study

The project began with a literature study to learn about the heart's function, ECGs, and which machine learning techniques that successfully detect arrhythmias from ECG signals. Once the initial investigation of techniques had been carried out, discussions with the collaboration company helped define which techniques and papers should be investigated in more detail. After the literature study, the main architecture of the CNN model in this project was determined.

4.2 Database and heartbeat segmentation

The AAMI standard described in Section 2.4 states that three datasets should be used for evaluation. According to the limitations of this project, one of these is used. The database used for training and evaluating the model in this project is the MIT-BIH Arrhythmia Database from PhysioNet [20], [21]. The data consists of 48 half-hour ECG recordings from 47 patients, hence two records are from the same patient. Of the 47 patients, there are 22 women and 25 men. The women are aged between 23 and 89 and the men are aged between 32 to 89. The ECG signals are digitized at 360 samples per second and all patients have ECG signals from two different leads. Most patients have a recording from the modified limb lead II (MLII). The other lead is usually the modified lead V1 but in some cases V2 or V5 and in one instance V4. Following AAMI, the patients annotated as 102, 104, 107, and 217 should be removed due to paced beats [24]. All the remaining 44 patients have signals from the MLII and therefore only signals from this lead were used as input to the model.

A time duration of 0.7 seconds of an ECG signal does generally cover all significant features of the heartbeat [35]. Each heartbeat in the database is annotated with a beat label and a timestamp. The aim of this project was to classify single heartbeat

arrhythmias. Therefore, the half-hour ECG signals provided by the database were segmented into individual heartbeats. In this thesis, each ECG signal of an individual heartbeat is 0.7 seconds. There are 0.25 seconds before the R-peak and 0.45 seconds after the peak.

4.3 Evaluation scheme

During the literature study it was found that in many of the published papers two evaluation schemes were used. They are denoted as the intra-patient scheme and the inter-patient scheme and Figure 4.1 presents an illustration of both schemes. The model developed in this project was evaluated according to the inter-patient scheme since it mimics the performance of the model in a real-world clinical setting.

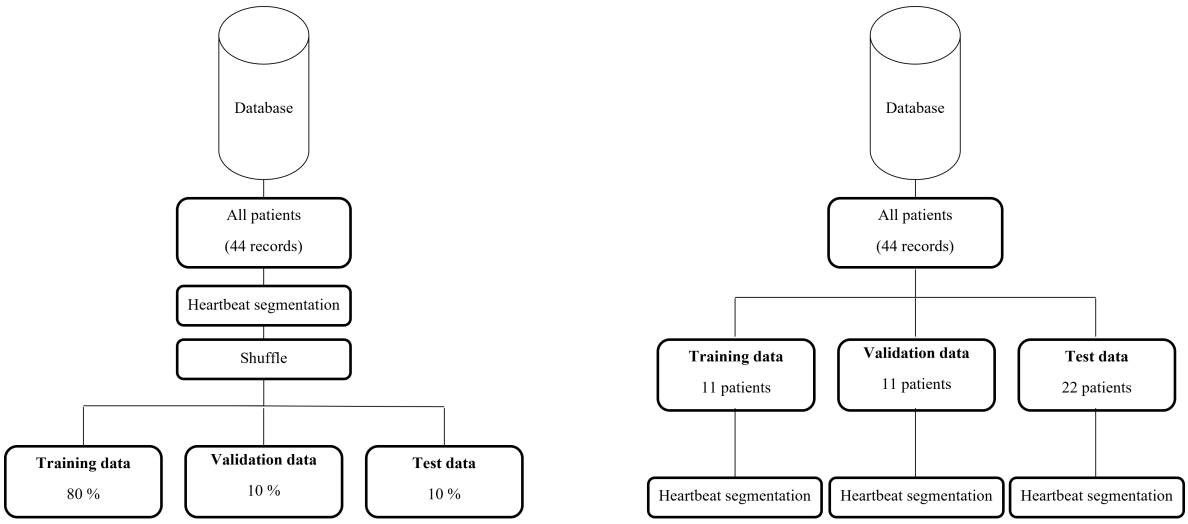

Figure 4.1: Illustration of the intra-patient and inter-patient evaluation schemes.

4.3.1 Intra-patient scheme

In the intra-patient scheme heartbeats from the same patients can be present in both the training set and test set. In the majority of articles covered in the literature study, the performance of the model was evaluated according to the intra-patient scheme. However, the intra-patient scheme produces biased results [10]. Heartbeats with almost identical characteristics will be present in both the training set and test set since heartbeats originating from the same patient will be present in both datasets. Models will learn the patient-specific characteristics and show high-performance results.

4.3.2 Inter-patient scheme

The inter-patient scheme is a scenario closer to reality compared to the intra-patient scheme. In the inter-patient scheme, the model trains on heartbeats from one group of patients and is evaluated on heartbeats from another group of patients. In this scenario the model is evaluated on a dataset, which for the model, consists of heartbeats from unseen patients [10]. Since this scheme represents a more realistic scenario it was chosen to be used when evaluating the model developed in this project.

A common division of the patients in the MIT-BIH Arrhythmia Database, using the inter-patient scheme, was introduced by Chazal, O'Dwyer, and Reilly [26]. Y. Li, Qian, and K. Li further developed this partition to also include a validation set by dividing patients from the original training set into a training and a validation group [27]. Table 4.1 illustrates the partition between patients used in this project.

Table 4.1: Partition of patients from the MIT-BIH Arrhythmia Database following an inter-patient evaluation scheme.

Dataset	**Patient in MIT-BIH Arrhythmia Database**
Training	101, 106, 108, 109, 114, 115, 116, 119, 122, 209, 223
Validation	112, 118, 124, 201, 203, 205, 207, 208, 215, 220, 230
Test	100, 103, 105, 111, 113, 117, 121, 123, 200, 202, 210, 212, 213, 214, 219, 221, 222, 228, 231, 232, 233, 234

Each dataset follows a similar distribution of non-ectopic (N), ventricular ectopic (V), and supraventricular ectopic (S) heartbeats to mimic realistic scenarios. According to Table 2.1, normal heartbeats are included in class N. Since most heartbeats of examined patients are normal, class N is considerably larger than all other classes. Bar plots for each dataset are shown in Figure 4.2. According to the limitations of the project three classes were used, N, S, and V, see Section 2.4. Therefore, the classes F and Q are extracted from the database.

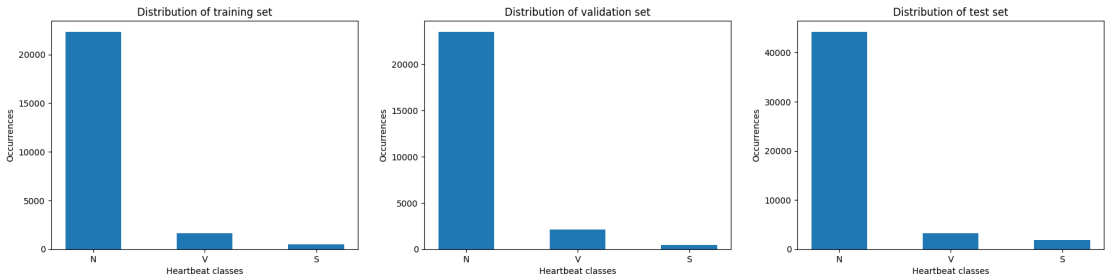

Figure 4.2: Distribution of heartbeats in the datasets.

4.4 The CNN model

The architecture of the CNN model used in this project was inspired by the research performed by Hannun *et al.* [6] and Sellami and Hwang [10]. The architecture of the CNN model is illustrated in Figure 4.3.

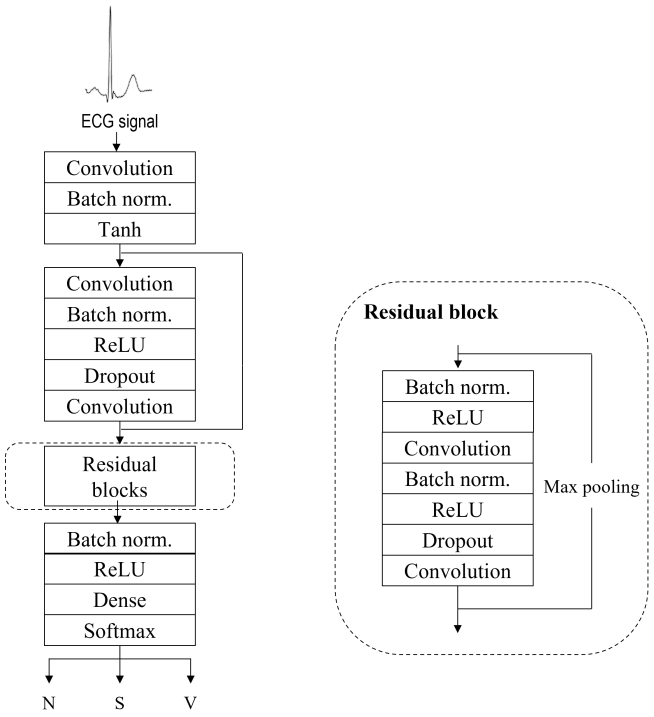

Figure 4.3: Illustration of the CNN model's architecture.

The number of residual blocks and dropout rate were decided by hyperparameter optimization and are described in detail in Section 4.4.1. The learning rate and batch size were set to 10^{-5} and 256, respectively.

The illustration in Figure 4.3 shows the residual blocks with a dashed line on the left hand side and a detailed architecture of one block is shown on the right hand side. The number of blocks is determined by the hyperparameter optimization. The size of the data is subsampled by a factor of two for every alternate residual block. The number of kernels for all convolutional layers within the residual blocks is $32 \cdot i$, where i starts at one and is incremented by one every fourth residual block.

Initially, ECG signals of single heartbeats were used as input to the CNN model. However, as shown by research performed by Sellami and Hwang [10], including the previous heartbeat as input to the model can help to classify the current heartbeat. This result was also observed in early simulations of the CNN model in this project. Once the previous heartbeat was included as input to the model the performance increased. The previous and current heartbeats were concatenated and fed as input to the model. Hence, the input became a $2 \cdot 0.7$ second long ECG signal. Figure 4.4 illustrates an example of an input to the CNN model.

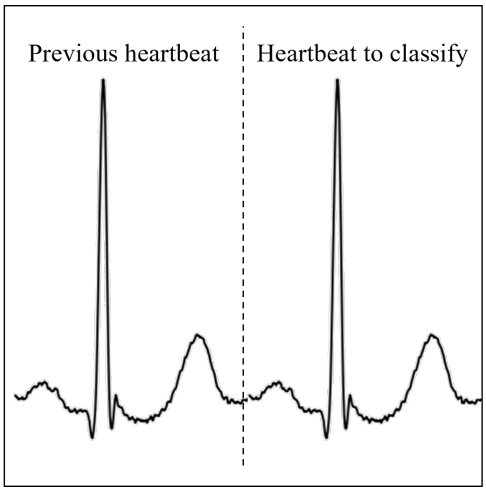

Figure 4.4: Illustration of an input to the CNN model. Plot of data from the MIT-BIH Arrhythmia Database.

4.4.1 Hyperparameter optimization

The number of residual blocks and the dropout rate for the CNN model presented in Section 4.4 were optimized. In the hyperparameter optimization, the values investigated for the number of residual blocks were 2, 4, 6, and 8 while the values for the dropout rate were 0, 0.2, and 0.4.

To determine the optimal setup all combinations between the number of residual blocks and the dropout rate were analyzed, hence twelve simulations were performed. For each combination, the model was trained on the training data and after each epoch evaluated on the validation set. Once the validation loss had not improved for five epochs the training was terminated in order to prevent overfitting. Figure 4.5 illustrates the cross entropy loss during training for one of the twelve simulations performed in the hyperparameter optimization. Figures for all twelve simulations are included in Appendix A.

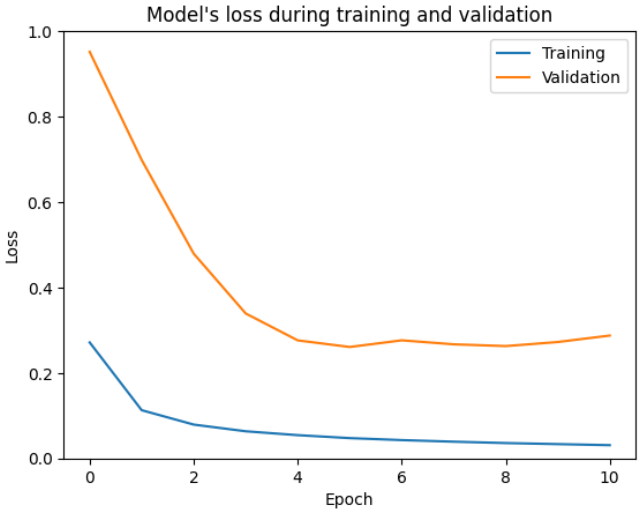

Figure 4.5: Training and validation progress of the CNN model with four residual blocks and a dropout rate of 0.

Table 4.2 summarizes the lowest validation loss achieved by each simulation. The CNN model with the lowest validation loss had eight residual blocks and a dropout rate of 0. Hence, this setup was determined to be used further on in this project.

Table 4.2: Lowest validation loss achieved during training in the hyperparameter optimization.

		Number of residual blocks			
		2	4	6	8
Dropout rate	0	0.33817	0.26076	0.29041	**0.22027**
	0.2	0.34329	0.30180	0.22940	0.28676
	0.4	0.37873	0.32337	0.25970	0.26204

4.4.2 Initial performance

The performance of the setup determined by the hyperparameter optimization, presented in Section 4.4.1 for the CNN model, presented in Section 4.4 was evaluated on the test data. Table 4.3 and 4.4 present this initial result.

Table 4.3: Initial performance for each heartbeat class.

Precision: N	**Recall: N**	**Precision: S**	**Recall: S**	**Precision: V**	**Recall: V**
0.95	1.00	0.22	0.00	0.97	0.78

Table 4.4: Confusion matrix for initial performance.

		Predicted label		
		N	S	V
True label	N	44 154	24	60
	S	1 819	7	11
	V	716	1	2 503

The result presented in Table 4.3 and 4.4 is adequate for non-ectopic (N) and ventricular ectopic (V) heartbeats. However, the result is inadequate for supraventricular (S) heartbeats.

To understand the model prediction, a two-dimensional representation of the ECG signal for each heartbeat was illustrated. Figure 4.6 shows a principal component analysis (PCA). PCA reduces the dimensionality of the ECG signals and displays it as points in a two dimensional plot and retains most of the variation in the dataset [36]. The PCA illustrates the difficulties in distinguishing between different classes. Class N and V seem separable while class S is more difficult to distinguish. The PCA plot does therefore reflect the performance in Table 4.3.

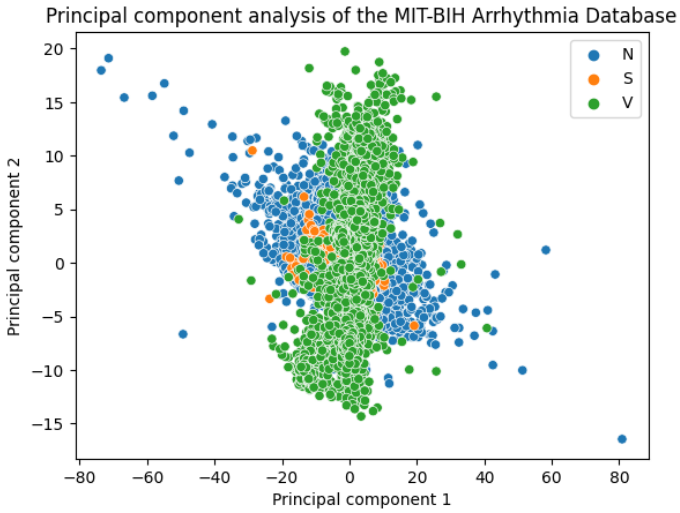

Figure 4.6: PCA visualization of the ECG signals in the database.

4.5 Ensemble learning

As presented in Section 4.4.2 the performance of class N and V are adequate while the performance of class S is inadequate. Hence, a method to improve the classification of class S is necessary. Investigating the confusion matrix presented in Table 4.3 it is shown that the most common miss-classification of class S is when the model predicts a heartbeat as N while the actual class is S.

A suggested method is to feed the network with additional information where class N and S become more distinguishable. By investigating the AAMI annotations, presented in Table 2.1, the heartbeats that belong to class S are different types of premature beats. A premature beat is a heartbeat that occurs earlier than expected [37]. Figure 2.3 illustrate that the target heartbeat of class S is premature but seems similar to class N in shape. Therefore, the time between two heartbeats can hold critical information required to identify class S.

4.5.1 Time dependence input

Inspired by Han *et al.* [25], time dependence as input to the model was introduced. In this project the time dependence, removed when segmenting the ECG signals, was added as input to the model using ensemble learning. Figure 4.7 presents how additional input with information about the time dependence is used in this project.

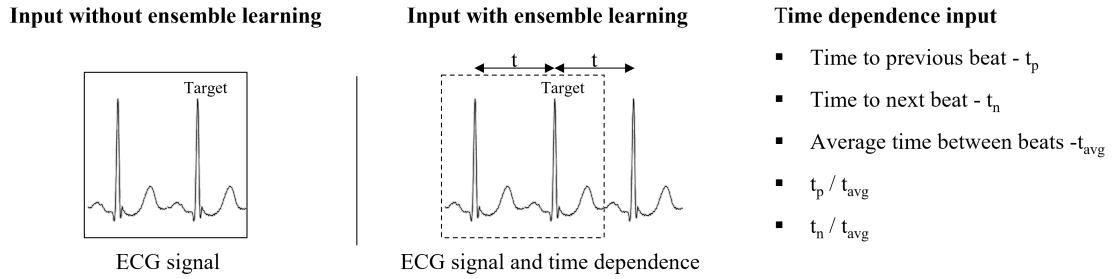

Figure 4.7: Illustration of the additional time dependence input for ensemble learning.

Figure 4.8 indicates how the clusters between the classes become more separable using the time dependence data. This strengthens how a model utilizing both the ECG signals and time dependence data as input could improve the performance of the model.

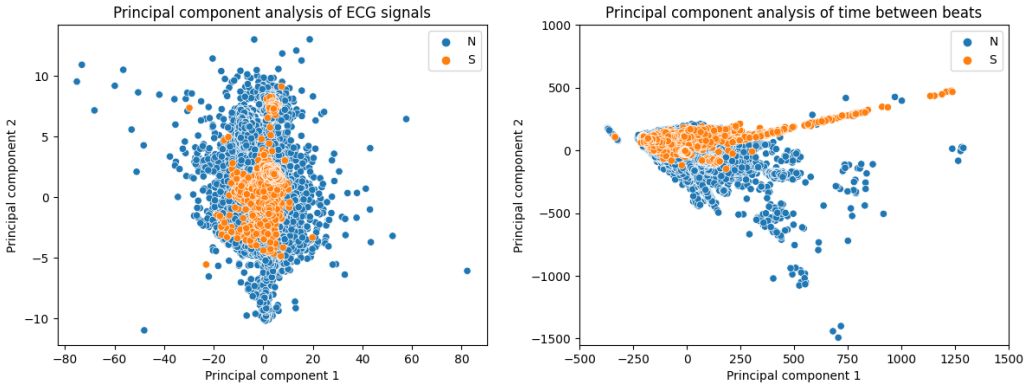

(a) PCA of ECG signals (b) PCA of time dependence data

Figure 4.8: PCA visualization of the differences between ECG signals and time dependence inputs for class N and S in the MIT-BIH Arrhythmia Database.

Ensemble learning is used to include both inputs. Figure 4.9 presents an overview of the proposed improved model utilizing ensemble learning. The multilayer perceptron (MLP) network and the ensemble method are presented in detail in Section 4.5.2, 4.5.3, respectively.

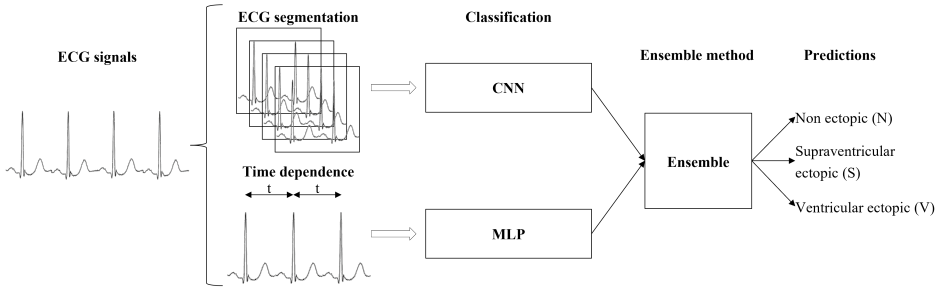

Figure 4.9: Illustration of the model utilizing ensemble learning.

4.5.2 Multi-layer perceptron model

A MLP network was created to distinguish between the classes N and S and was fed with time dependence data as input. To determine a suitable architecture, various MLP networks were trained using time dependence data from class N and S. No hyperparameter optimization was done for the MLP model. Table 4.5 shows the architecture of the MLP network yielded the lowest validation loss.

Table 4.5: Architecture of the MLP model.

Layer	Number of neurons	Activation function
Fully connected 1	16	Relu
Fully connected 2	64	Relu
Fully connected 3	16	Relu
Fully connected 4	1	Relu

4.5.3 Ensemble method

The ensemble method for this project is based on the hierarchy between the CNN model and the MLP model. Since the CNN model presented in Section 4.4 achieved an adequate result for class V, this model is used to classify heartbeats of class V while the MLP model is used to classify heartbeats of class N and S. Figure 4.10 illustrates a scheme over the ensemble method used in this project.

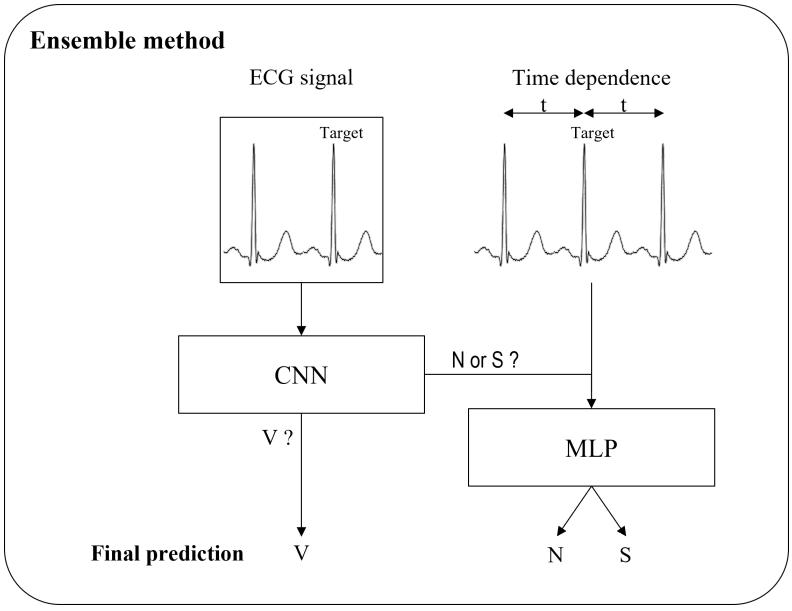

Figure 4.10: Illustration of the hierarchical ensemble method structure.

5

Results

This chapter presents the performance of the proposed model developed in Chapter 4. The inter-patient evaluation scheme, presented in Section 4.3, was used to mimic real-world clinical settings. The learning rate was set to 10^{-5} and the batch size was set to 256 for all results. From the hyperparameter optimization presented in Section 4.4.1 the CNN model with the lowest validation loss had eight residual blocks and a dropout rate of 0.

5.1 Training and validation

Figure 5.1 presents the training and validation progress of the CNN model and the MLP model.

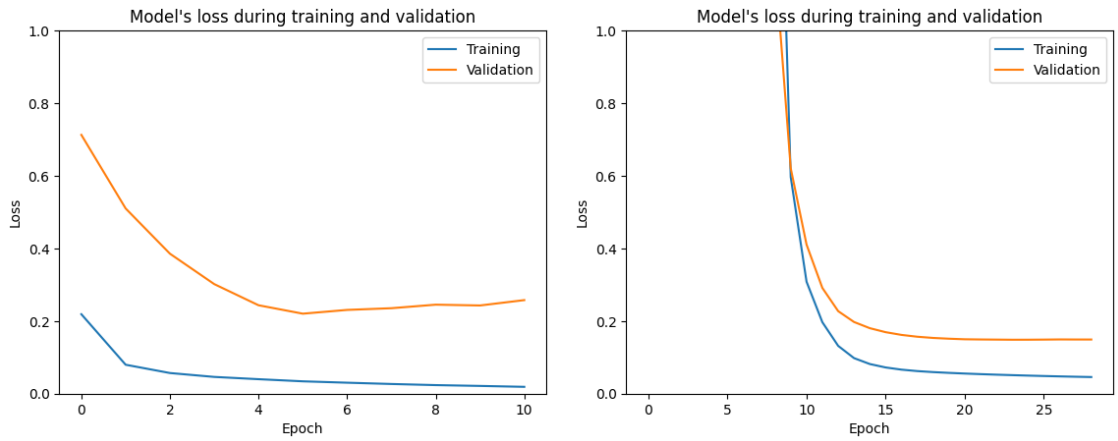

(a) CNN model

(b) MLP model

Figure 5.1: Training and validation progress of the optimized CNN model and the MLP model.

5.2 Test performance

The CNN and MLP models were combined with ensemble learning as described in Section 4.5 and were evaluated on the test set. The confusion matrix of the predictions on the test set is presented in Table 5.1.

Table 5.1: Confusion matrix of the proposed model's predictions on the test data.

		Predicted label		
		N	S	V
True label	N	42 787	1 391	60
	S	684	1 142	11
	V	692	25	2 503

Table 5.2 presents the performance of the proposed model and related research that has used the same test set.

Table 5.2: Performance of the proposed model compared to related machine learning models.

Authors	**Precision: N**	**Recall: N**	**Precision: S**	**Recall: S**	**Precision: V**	**Recall: V**
Li *et al.* [27]	93 %	95 %	66 %	35 %	80 %	88 %
Sellami *et al.* [10]	99 %	89 %	30 %	82 %	72 %	92 %
Han *et al.* [25]	100 %	96 %	47 %	88 %	83 %	94 %
Proposed model	97 %	97 %	45 %	62 %	97 %	78 %

6

Discussion

This chapter contains a discussion of the results obtained. Further, ethical considerations regarding utilizing machine learning in the healthcare domain are presented. Finally, this chapter covers further development of this project and describes potential future work.

6.1 Dataset

The initial aim of this project was to interpret signals from the mobile ECG device manufactured by the collaboration company. A large number of patients were supposed to wear the ECG device for several days and ECG signals from each heartbeat were supposed to be gathered. However, regulation delayed the process of gathering data from the mobile ECG device. To overcome this, data from a public database was used. The project became a preparation for when the wearable data has been gathered. It is thought that the methodology developed in this project is suitable to be used also on data from the wearable device.

The MIT-BIH Arrhythmia Database was used for this project. The database contains ECG signals from 44 patients, see Section 4.2. In the context of machine learning this is a small amount of data. For comparison, the research performed by Hannun *et al.* [6] had access to ECG signals from 53 549 different patients. Access to more data is thought to improve the performance. Therefore, for further improvements, ECG signals from more patients should be used.

A common dataset division for training machine learning models is around 80 %, 10 %, and 10 % for training, validation, and test data, respectively. According to the methodology presented by [27] the division of patients follows Table 4.1, where the training set and the validation set consist of 11 patients each while the test set contains the remaining 22 patients. Initially, the number of patients in the training and validation set for this project was elaborated to follow a more common division and improve the model's learning by increasing the number of patients in the training set. The investigated division had 17 patients in the training set and 5 patients in the validation set. The patients that were moved to the training set were chosen so that the ratio between the different classes should remain unaffected over the data sets as in Figure 4.2. To still be able to compare the performance

with other studies the test set was the same as presented in Table 4.1. Simulations with this division indicated that a larger validation set was required so therefore the division presented in Table 4.1 was used in this project.

The elaborations with the dataset division indicated that the ECG morphology of heartbeats annotated with the same class differentiates between patients. Figure 6.1 strengthens this indication. The figure illustrates a T-Distributed Stochastic Neighbor Embedding (T-SNE) visualization representing non-ectopic (N) heartbeats from four different patients. T-SNE uses conditional probabilities of the high-dimensional distances between data points and tries to minimize the Kullback-Leibler divergences [38].

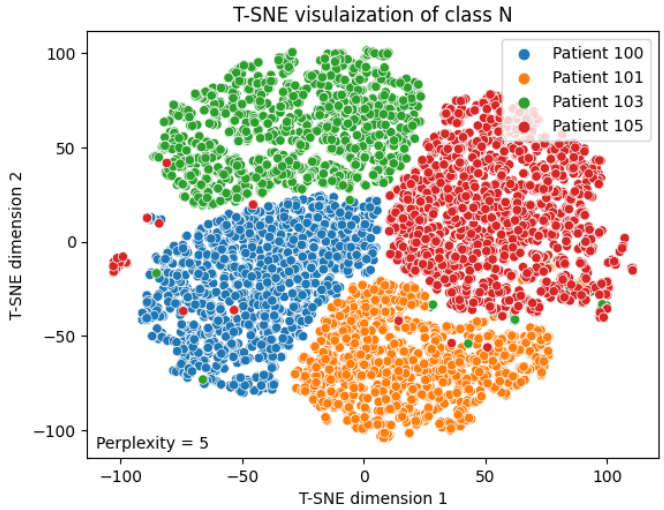

Figure 6.1: T-SNE visualization of non-ectopic (N) heartbeats from four patients in the MIT-BIH Arrhythmia Database.

Since the ECG morphology differentiates between patients a small validation set might therefore not be representative to validate the data during training and the model's performance between the validation set and the test set can differentiate significantly. This scenario becomes more unlikely for larger validation sets since the weights must fit more patients' heartbeats.

6.2 Reproducibility of results

Initially, each simulation of the CNN network, with the same parameter setup, obtained slightly different results. An explanation for this could be the usage of random initialization of the weights which was initially used. If the dataset is large, the initial weight randomization should not affect the outcome of the network since it should converge to the same optimal weights. However, for a small dataset, as in this project, the initial weight difference can affect the outcome. To avoid the difference between simulations a seed initialization of the weights was introduced. A seed ensures that the weights have the same initialization for each simulation. This

was important to obtain equal evaluations during the hyperparameter optimization. The optimized hyperparameters might not be optimal for all seeds. For another seed the outcome of the hyperparameter optimization might differentiate from the one obtained in this thesis.

6.3 Ethical considerations

Applying machine learning in the healthcare domain opens a wide range of possibilities. Machine learning has the potential to minimize the number of misdiagnoses, reduce costs, and facilitate health care decisions and thereby democratize healthcare. However, there are challenges that must be considered before implementation in real-world clinical settings.

New regulations must be defined to handle potential misdiagnoses made by a model. Healthcare workflow and responsibilities must be redefined so that they cover the usage of algorithms, for what clinical context, and when it should aid decision making.

One ethical aspect is to define the trade-off between precision and recall. According to the definition of recall, Eq 3.3, the value will increase when the number of false negative decreases. According to the definition of precision, Eq 3.2, the value will increase when the number of false positive decreases. Low recall can have fatal consequences since the model is then unable to detect arrhythmias when they are actually present. On the other hand, low precision results in reporting more arrhythmias than there actually are. Low precision hence results in financial costs and requires cardiologists or other healthcare professionals to unnecessarily examine patients as well as increasing the anxiety of patients.

Companies developing machine learning models for the healthcare domain have a strong influence over the models' decisions and thereby the trade-off between precision and recall, which to some extent represents the trade-off between financial costs and the health of patients.

6.4 Future work

First, important future work is to train and test the proposed model on a larger dataset. In this project, due to lack of data, the model was trained and evaluated on the MIT-BIH Arrhythmia Database. Hence, as a future project, data from an ECG device should be gathered and used to train the model before it is evaluated on three public databases. To completely follow regulations the model should be evaluated on the full MIT-BIH Arrhythmia Database and two other public databases, see Section 2.4.

Second, this proposed model could be further developed to analyze ECG signals from several leads. In hospitals, 12 leads are analyzed to diagnose the cardiovascular status of a patient. In this project, ECG signals from one lead were used as input

to the model, see Section 4.2. Utilizing several leads as input might give the model additional valuable information and increase the performance of the model.

Finally, the objective of this project was to develop an algorithm detecting single heartbeat arrhythmias. A limitation is that the model cannot classify any rhythmic arrhythmias or single heartbeat arrhythmias of class F and Q, see Section 1.3. A model detecting all single heartbeat arrhythmias and rhythmic arrhythmias could be developed as a future project.

7

Conclusion

The proposed model design included ensemble learning between a convolutional neural network and a multilayer perceptron network. The model was trained and evaluated on the MIT-BIH Arrhythmia Database and was able to classify ectopic heartbeat arrhythmias into three classes. The model achieved a precision score of 97 %, 45 %, and 97 % and a recall score of 97 %, 62 %, and 78 % for non-ectopic (N), supraventricular ectopic (S), and ventricular ectopic (V) heartbeats, respectively.

ECG signals of single heartbeats yielded adequate results for classifying ventricular ectopic heartbeats which can be explained by the fact that they often differentiate from non-ectopic heartbeats in shape. It was also shown that ECG signals of single heartbeats were not enough as input to yield adequate results for classifying supraventricular ectopic heartbeats. In addition, it was shown that by using time dependence data as additional input and utilizing ensemble learning the model could classify supraventricular ectopic heartbeats to a higher extent.

This thesis strengthens that machine learning models can be used to detect and classify single heartbeat arrhythmias from ECG signals.

Bibliography

[1] World Healt Organization, "Cardiovascular diseases (CVDs)," 2023. [Online]. Available: https://www.who.int/news-room/fact-sheets/detail/cardiovascular-diseases-(cvds) (accessed Jan. 1, 2023).

[2] X.-L. Yang, G.-Z. Liu, Y.-H. Tong, *et al.*, "The history, hotspots, and trends of electrocardiogram," *Journal of Geriatric Cardiology*, vol. 12, no. 4, pp. 448–456, Jul. 2015. DOI: 10.11909/j.issn.1671-5411.2015.04.018.

[3] W. Brady, *Electrocardiogram in Clinical Medicine*. John Wiley & Sons, Inc., 2020, ch. 1, 2, pp. 3–11, 13–17.

[4] A. Davies, M. Vigo, S. Harper, and C. Jay, "The visualisation of eye-tracking scanpaths: What can they tell us about how clinicians view electrocardiograms?" In *2016 IEEE Second Workshop on Eye Tracking and Visualization (ETVIS)*, 2016, pp. 79–83. DOI: 10.1109/ETVIS.2016.7851172.

[5] E. J. da S. Luz, W. R. Schwartz, G. Cámara-Chávez, and D. Menotti, "Ecg-based heartbeat classification for arrhythmia detection: A survey," *Computer Methods and Programs in Biomedicine*, vol. 127, pp. 144–164, Apr. 2016. DOI: 10.1016/j.cmpb.2015.12.008.

[6] A. Y. Hannun, P. Rajpurkar, M. Haghpanahi, *et al.*, "Cardiolgist-level arrhythmia detection and classification in ambulatory electrocardiograms using a deep neural network," *Nature Medicine*, vol. 25, no. 4, pp. 65–69, Jan. 2019. DOI: 10.1038/s41591-018-0268-3.

[7] M. A. Serhani, H. T. E. Kassabi, H. Ismail, and A. N. Navaz, "Ecg monitoring systems: Review, architecture, processes, and key challenges," *Sensors*, vol. 20, no. 6, p. 1796, Mar. 2015. DOI: 10.3390/s20061796.

[8] Z. I. Attia, D. M. Harmon, E. R. Behr, and P. A. Friedman, "Application of artificial intelligence to the electrocardiograms," *Eur Heart J.*, vol. 42, no. 46, pp. 4717–4730, 2015. DOI: 10.1093/eurheartj/ehab649.

[9] Z. Ebrahimi, M. Loni, M. Daneshtalab, and A. Gharehbaghi, "A review on deep learning methods for ecg arrhythmia classification," *Expert Systems with Applications: X*, vol. 7, Sep. 2020. DOI: 10.1016/j.eswax.2020.100033.

[10] A. Sellami and H. Hwang, "A robust deep convolutional neural network with batch-weighted loss for heartbeat classification," *Expert Systems With Applications*, vol. 122, pp. 75–84, 2019. DOI: 10.1016/j.eswa.2018.12.037.

[11] ECG & ECHO Learning, "Cardiac electrophysiology and ECG interpretation," 2023. [Online]. Available: https://ecgwaves.com/topic/introduction-electrocardiography-ecg-book/ (accessed Jun. 4, 2023).

[12] Cleveland Clinic, "Heart Conduction System," 2023. [Online]. Available: https://my.clevelandclinic.org/health/body/21648-heart-conduction-system (accessed Feb. 14, 2023).

[13] E. Ashley and J. Niebauer, "Conquering the ecg," in *Cardiology Explained*. Remedica, 2004, ch. 3.

[14] R. H. Md, "Anatomy of the Heart," 2023. [Online]. Available: https://commons.wikimedia.org/w/index.php?curid=68483372 (accessed Jun. 6, 2023).

[15] A. B. De Luna, V. N. Batchvarov, and M. Malik, "The morphology of the electrocardiogram," *The ESC Textbook of Cardiovascular Medicine Blackwell Publishing*, vol. 35, 2006.

[16] ECG & ECHO LEARNING, "THe ECG leads: electrodes, limb leads, chest (precordial leads, 12-Lead ECG (EKG))", ECG & ECHO LEARNING, Accessed 30-03-2023 [Online]. Available: https://ecgwaves.com/topic/ekg-ecg-leads-electrodes-systems-limb-chest-precordial/.

[17] National Heart, Lung, and Blood Institute, "'What Is an Arrhythmia?," 2023. [Online]. Available: https://www.nhlbi.nih.gov/health/arrhythmias (accessed Mar. 29, 2023).

[18] A. H. Kuruwita, N. S. Kay, A. Liew, *et al.*, "Ectopic heartbeat detection from ecg signals using deep convolutional neural networks," in *2022 IEEE International Conference on Bioinformatics and Biomedicine (BIBM)*, 2022, pp. 3535–3540. DOI: 10.1109/BIBM55620.2022.9995477.

[19] Cleveland Clinic, "Ectopic Heartbeat," 2023. [Online]. Available: https://my.clevelandclinic.org/health/diseases/23000-ectopic-heartbeat (accessed Jun. 4, 2023).

[20] G. Moody and R. Mark, "The impact of the mit-bih arrhythmia database," *IEEE Engineering in Medicine and Biology Magazine*, vol. 20, no. 3, pp. 45–50, 2001. DOI: 10.1109/51.932724.

[21] A. Goldberger, L. Amaral, L. Glass, *et al.*, "Physiobank, physiotoolkit, and physionet: Components of a new research resource for complex physiologic signals," *Circulation*, vol. 101, no. 23, e215–e220, 2000. DOI: 10.1161/01.cir.101.23.e215.

[22] G. Sannino and G. De Pietro, "A deep learning approach for ecg-based heartbeat classification for arrhythmia detection," *Future Generation Computer*

Systems, vol. 86, pp. 446–455, 2018. DOI: https://doi.org/10.1016/j.future.2018.03.057.

[23] U.S. Food & Drug Administration, "Arrhythmia Detector and Alarm - Class II Special Controls Guidance Document for Industry and FDA Staff," 2023. [Online]. Available: https://www.fda.gov/medical-devices/guidance-documents-medical-devices-and-radiation-emitting-products/arrhythmia-detector-and-alarm-class-ii-special-controls-guidance-document-industry-and-fda-staff#10 (accessed Jan. 2, 2023).

[24] American National Standards Institute, "Testing and reporting performance results of cardiac rhythm and ST segment measurement algorithms," 2023. [Online]. Available: https://webstore.ansi.org/standards/aami/ansiaamiec572012 (accessed Jan. 20, 2023).

[25] C. Han, P. Wang, R. Huang, and L. Cui, "Hctnet: An experience-guided deep learning network for inter-patient arrhythmia classification on imbalanced dataset," vol. 78, 2022. DOI: 10.1016/j.bspc.2022.103910.

[26] P. de Chazal, M. O'Dwyer, and R. Reilly, "Automatic classification of heartbeats using ecg morphology and heartbeat interval features," *IEEE Transactions on Biomedical Engineering*, vol. 51, no. 7, pp. 1196–1206, 2004. DOI: 10.1109/TBME.2004.827359.

[27] Y. Li, R. Qian, and K. Li, "Inter-patient arrhythmia classification with improved deep residual convolutional neural network," *Computer Methods and Programs in Biomedicine*, vol. 214, 2022. DOI: 10.1016/j.cmpb.2021.106582.

[28] B. Mehlig, *Machine Learning with Neural Networks: An Introduction for Scientists and Engineers*. Cambridge University Press, 2021, ch. 5, 7 and 8, 75–95, 114-140 and 141–156. DOI: 10.1017/9781108860604.

[29] IBM, "Convolutional Neural Networks," 2023. [Online]. Available: https://www.ibm.com/topics/convolutional-neural-networks (accessed Feb. 28, 2023).

[30] S. Albawi, T. A. Mohammed, and S. Al-Zawi, "Understanding of a convolutional neural network," in *2017 International Conference on Engineering and Technology (ICET)*, 2017, pp. 1–6. DOI: 10.1109/ICEngTechnol.2017.8308186.

[31] O. Sagi and L. Rokach, "Ensemble learning: A survey," *Wires data mining and knowledge discovery*, vol. 8, no. 4, 2018. DOI: 10.1002/widm.1249.

[32] A. P. Bradley, "The use of the area under the roc curve in the evaluation of machine learning algorithms," *Pattern Recognition*, vol. 30, no. 7, pp. 1145–1159, 1997. DOI: 10.1016/S0031-3203(96)00142-2.

[33] D. K. Sharma, M. Chatterjee, G. Kaur, and S. Vavilala, "Deep learning applications for disease diagnosis," in *Deep Learning for Medical Applications with Unique Data*. Elsevier, 2022, ch. 3, pp. 31–51. DOI: 10.1016/B978-0-12-824145-5.00005-8.

[34] M. Grandini, E. Bagli, and G. Visani, "Metrics for multi-class classification: An overview.," 2020. [Online]. Available: https://search.ebscohost.com/login.aspx?direct=true&db=edsarx&AN=edsarx.2008.05756&site=eds-live&scope=site&authtype=guest&custid=s3911979&groupid=main&profile=eds.

[35] K. Ramasamy, K. Balakrishnan, and D. Velusamy, "Detection of cardiac arrhythmias from ecg signals using fbse and jaya optimized ensemble random subspace k-nearest neighbor algorithm," *Biomedical Signal Processing and Control*, vol. 76, p. 103 654, 2022. DOI: 10.1016/j.bspc.2022.103654.

[36] M. Ringnér, "What is principal component analysis?" *Nature Biotechnology*, vol. 26, pp. 303–304, 2008. DOI: https://doi.org/10.1038/nbt0308-303.

[37] M. Gusev, "Detection of premature heartbeats," in *2022 45th Jubilee International Convention on Information, Communication and Electronic Technology (MIPRO)*, 2022, pp. 350–355. DOI: 10.23919/MIPRO55190.2022.9803747.

[38] L. van der Maaten and G. Hinton, "Visualizing data using t-sne," *Journal of Machine Learning Research*, vol. 9, no. 11, pp. 2579–2605, 2008.

A

Appendix 1

All simulations in the hyperparameter optimization described in Section 4.4.1 are presented in this Appendix.

A.1 Two residual blocks

Figure A.1: Two residual blocks and a dropout rate of 0.

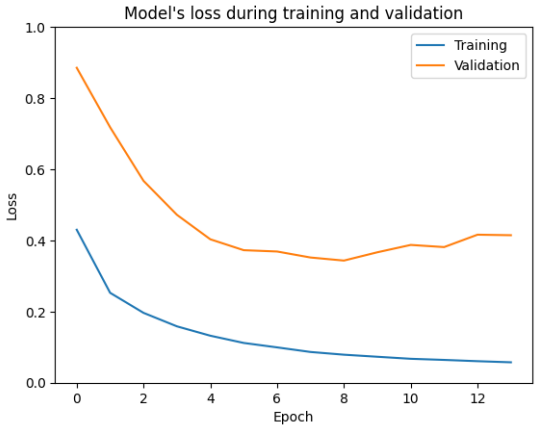

Figure A.2: Two residual blocks and a dropout rate of 0.2.

Figure A.3: Two residual blocks and a dropout rate of 0.4.

A.2 Four residual blocks

Figure A.4: Four residual blocks and a dropout rate of 0.

Figure A.5: Four residual blocks and a dropout rate of 0.2.

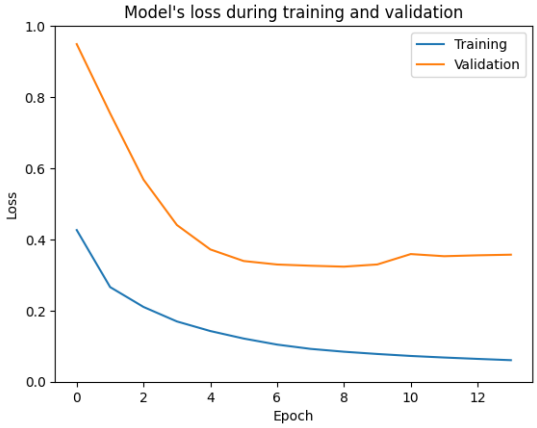

Figure A.6: Four residual blocks and a dropout rate of 0.4.

A.3 Six residual blocks

Figure A.7: Six residual blocks and a dropout rate of 0.

Figure A.8: Six residual blocks and a dropout rate of 0.2.

Figure A.9: Six residual blocks and a dropout rate of 0.4.

A.4 Eight residual blocks

Figure A.10: Eight residual blocks and a dropout rate of 0.

Figure A.11: Eight residual blocks and a dropout rate of 0.2.

Figure A.12: Eight residual blocks and a dropout rate of 0.4.

DEPARTMENT OF PHYSICS
CHALMERS UNIVERSITY OF TECHNOLOGY
Gothenburg, Sweden
www.chalmers.se

CHALMERS
UNIVERSITY OF TECHNOLOGY